Pastes and hydrogels from carboxymethyl cellulose sodium salt as supporting electrolyte of solid electrochemical supercapacitors

Maria M. Pérez-Madrigal,[1,*] Miquel G. Edo,[1] Maricruz G. Saborío,[1,2] Francesc Estrany[1,2] and Carlos Alemán[1,2,*]

[1] *Departament d'Enginyeria Química, EEBE, Universitat Politècnica de Catalunya, C/ Eduard Maristany 10-14, Ed. I2, 08019 Barcelona, Spain*

[2] *Barcelona Research Center for Multiscale Science and Engineering, Universitat Politècnica de Catalunya, Eduard Maristany 10-14, 08019 Barcelona, Spain*

[*] m.mar.perez@upc.edu and carlos.aleman@upc.edu

ABSTRACT

Different carboxymethyl cellulose sodium salt (NaCMC)-based pastes and hydrogels, both containing a salt as supporting electrolyte, have been prepared and characterized as potential solid state electrolyte (SSE) for solid electrochemical supercapacitors (ESCs).The characteristics of the NaCMC-based SSEs have been optimized by examining the influence of five different factors in the capacitive response of poly(3,4-ethylenedioxythiophene) (PEDOT) electrodes: *i)* the chemical nature of the salt used as supporting electrolyte; *ii)* the concentration of such salt; *iii)* the concentration of cellulose used to prepare the paste; *iv)* the concentration of citric acid employed during NaCMC cross-linking; and *v)* the treatment applied to recover the supporting electrolyte after washing the hydrogel. The specific capacitance of the device prepared using the optimized hydrogel as SSE is 81.5 and 76.8 F/g by means of cyclic voltammetry and galvanostatic charge/discharge, respectively, these values decreasing to 60.7 and 75.5 F/g when the SSE is the paste.

Keywords: Biosupercapacitors; Cell voltage; Batteries; Poly(3,4-ethylenedioxythiophene); Specific capacitance

Abbreviations:

ESC: electrochemical supercapacitor

CV: cyclic voltammetry

GCD: galvanostatic charge/discharge

LC: leakage current

NaCMC: carboxymethyl cellulose sodium salt

PEDOT: poly(3,4-ethylenedioxythiophene)

SC: specific capacitance

SD: self-discharging

SR: swelling ratio

SSE: solid state electrolyte

η: Coulombic efficiency

INTRODUCTION

During the last decade, the urgent need to replace fossil fuels and alleviate the climate change problem has entailed unprecedented attention and efforts towards the development of alternative energy sources and energy storage devices. Currently, supercapacitors, whose working mechanism is based on electrostatic charge accumulation at interfaces between electrodes and electrolyte ions, are considered as energy storage devices with a great potential due to their high-power, long cycle life, low maintenance cost, and safe pollution-free operation (Chen, Xu, Wei, & Yang, 2016; Hibino, Kobayashi, Nagao, & Kawasaki, 2015; Zhou, Ye, Wan, & Jia, 2015). These advantages promote the use of supercapacitors in a large variety of applications, as for example motor vehicles (Kühne, 2010; Miller, & Simon, 2008; Rezzak, & Boudjerda, 2017), laptops (Gao et al., 2011) autonomous medical sensors (Guo et al, 2017), wearable electronics (Bao, & Li, 2012; Jost et al., 2013), and energy harvesters (Pavković, Hoić, Deur, & Petrić, 2014; Yuan et al, 2012).

Depending on the energy-storage mechanism, electrode materials are divided in two different main groups (Conway, 1999). In the first one (called *double layer capacitors*) the capacitive behavior solely relies on the electrostatic interactions (adsorption) between electrolytic ions and the electrode surface (*i.e.* electrical double-layer capacitance), while faradaic reactions contribute to the overall capacitance (*i.e.* pseudocapacitance) in the second group (known as *pseudocapacitors*). Electroactive conducting polymers and metal oxides belong to the latter group, while porous carbon materials, as for example graphene and carbon nanotubes, are typically used for double layer supercapacitors.

Solid electrochemical supercapacitors (ESCs) that contain biodegradable polymers from renewable natural sources have become a topic of great interest. These

biopolymers are typically used in the electrodes (Armelin, Pérez-Madrigal, Alemán, & Díaz, 2016a; Cui et al., 2014; Hamedi et al., 2014; Mondal, Perween, Srivastava, & Ghosh, 2014; Saborío et al., 2018; Zhang et al., 2015; Zheng, Cai, Ma, & Gong, 2015), imparting lightweight and flexibility, or as solid state electrolyte (SSE), acting as a reservoir of absorbed electrolytes (Armelin et al., 2016; Cao et al., 2017; Gao et al., 2013a; Gui et al. 2013; Lee et al., 2017; Mantravadi, Chinnam, Dikin, & Wunder, 2016; Pérez-Madrigal, Estrany, Armelin, Díaz-Díaz, & Alemán, 2016a; Pérez-Madrigal, Edo, Díaz, Puiggalí, Alemán, 2017). Indeed, polymers from natural sources offer challenging opportunities in the development of renewable, sustainable, cheap and scalable charge storage devices because of their unique properties and low cost. Among those, cellulose is the most abundant and sustainable among natural polymers. Specifically, cellulose fibers exhibit high aspect ratios, high surface area, high porosity, excellent mechanical properties, excellent flexibility, and the ability to bind to other conductive materials, thus enabling extensive application in flexible energy-storage devices, as it has been recently reviewed (Nyholm, Nyström, Mihranyan, & Strømme, 2011; Pérez-Madrigal et al., 2017; Wang, Tammela, Strømme, & Nyholm, 2017; Wang, Yao, Wang, & Li, 2017).

Cellulose-based materials have been widely employed as support for mechanical reinforcement (Fei, Yang, Bao, & Wang, 2014; Håkansson et al., 2016; Liu et al., 2014; Lu, Yu, Wang, Tong, & Li, 2014; Nyholm et al., 2011; Pérez-Madrigal, Edo, & Alemán, 2016b; Pérez-Madrigal et al., 2017; Wang et al., 2017; Wang et al., 2017) since the good mechanical properties of this polysaccharide confer mechanical strength and/or flexibility to the electrode. For instance, cellulose is used as structural scaffold for depositing active conducting materials. In addition, other interesting properties, such as transparency, chemical stability, and light weight, can be indirectly obtained in some

cases. However, the role of cellulose as SSE has been indirectly and scarcely studied (Gao et al., 2013a; Gao et al., 2013b; Gui et al., 2013; Mantravadi, Chinnam, Dikin, & Wunder, 2016; Sudhakar, Bhat, Selvakumar, 2016). Gui et al. (2013) studied the electrolyte absorption properties of cellulose fibers, which transported electrolyte ions via the pores from bulk baths to the energy-active material. Flexible cellulose nanofibers were also selected as aqueous electrolyte nanoreservoirs and nanospacers for graphene- and carbon nanotubes-based electrode materials (Gao et al., 2013a; Gao et al., 2013b). From another perspective, strong and solid polymer electrolyte ion gels composed of methyl cellulose fibers were prepared, even though their application in electrochemical supercapacitors and their effects in the electrochemical stability of electroactive electrodes were not tested (Mantravadi et al., 2016). Finally, Sudhakar et al. (2016) prepared an eco-friendly and transparent SSE using cellulose acetate propionate, H_3PO_4, and poly(ethylene glycol), which acted as plasticizer. The performance of this cellulose-containing SSE was evaluated mixing activated carbon with a binder to form a slurry, which was subsequently screen printed coated onto stainless steel electrodes. The resulting supercapacitor showed a specific capacitance of 64 F/g and a stability of 96% after 1000 charge-discharge cycles.

In this work we examine the performance of pastes (extremely high viscous aqueous solutions) and hydrogels, which were prepared using carboxymethyl cellulose sodium salt (NaCMC; Scheme 1), as novel and sustainable SSEs for compact ESCs manufactured with poly(3,4-ethylenedioxythiophene) (PEDOT) electrodes, hereafter denoted PEDOT/NaCMC ESCs. It is worth noting that cellulose, which is the most abundant and sustainable natural polymer, is insoluble in water. In contrast, the cellulose ether, NaCMC, which obtained attacking the alkali cellulose, is soluble and dispersible in water to form highly viscous solutions useful for the formation of pastes,

hydrogels, and even films (by evaporation of water). After characterization of cellulose-based pastes and hydrogels, their response as SSEs was enhanced by adding salts, which acted as supporting electrolyte. In particular, the influence of several parameters in the capacitive properties of PEDOT/NaCMC ESCs has been carefully analyzed. Such parameters include the chemical nature of the absorbed salt (NaCl, KCl, $CaCl_2$, Na_2HPO_4 or Na_2SO_4), the concentration of supporting electrolyte, the cellulose concentration, the cross-linking degree, and the post-washing treatment. Finally, the cyclability and the capacitive, self-discharging and leakage-current responses of the ESCs with optimized NaCMC-based SSEs have been investigated.

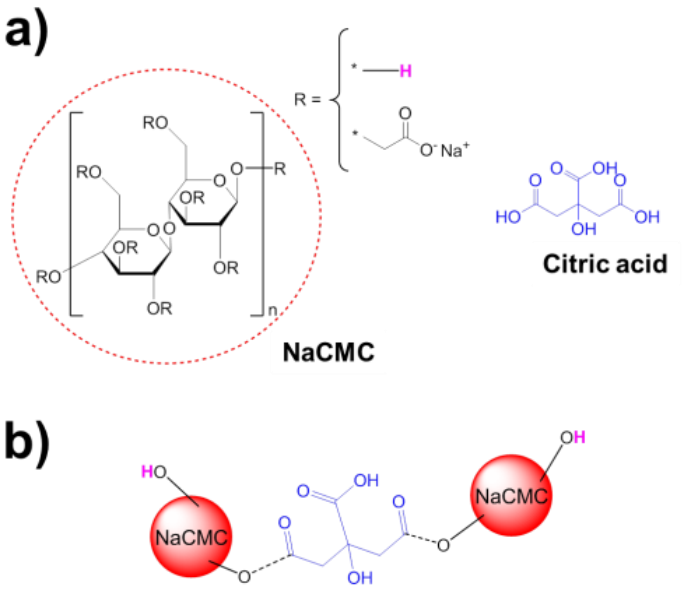

Scheme 1: a) Chemical structure of the components of cellulose hydrogels prepared in this work; b) Cross-linking of NaCMC chains with citric acid.

METHODS

Materials

All reagents were used as purchased without further purification. For the synthesis of PEDOT electrodes, acetonitrile (Reag. Ph. Eur. for analysis, ACS) was purchased from Panreac (Spain), and 3,4-ethylenedioxythiophene (EDOT, 97%) and $LiClO_4$ (ACS

reagent, ≥ 95.0%; stored in an oven at 70 °C before use) were purchased from Sigma-Aldrich. NaCMC with high viscosity (1500-3000 cP, 1 % in H_2O at 25 °C), citric acid (99%), and sodium azide (NaN_3 ≥99.5%) were purchased from Sigma-Aldrich. The list of salts evaluated as supporting electrolyte in NaCMC-based SSEs includes: NaCl (Panreac), KCl (Merck), $CaCl_2$ (Scharlab), Na_2HPO_4 (Panreac), and Na_2SO_4 (Scharlau).

Preparation of PEDOT electrodes

PEDOT electrodes were prepared by methods already described (Pérez-Madrigal et al., 2016a; Pérez-Madrigal et al., 2017). Briefly, PEDOT was obtained by anodic polymerization in acetonitrile at a constant potential of 1.25 V imposing a polymerization charge equal to 500 mC/cm^2 (at room temperature and nitrogen atmosphere). The mass of PEDOT deposited onto the WE (m_{pol}= 1.143 ± 0.097 mg) was determined as the weight difference between coated and uncoated steel sheets (n = 26) using a CPA26P Sartorius analytical microbalance with a precision of 10^{-6} g. Complete characterization of the resulting PEDOT electrodes was previously reported (Pérez-Madrigal et al., 2016a; Pérez-Madrigal et al., 2017).

Preparation of cellulose pastes and biohydrogels

NaCMC pastes and hydrogels were prepared adapting a procedure described (Jiang, Gao, Wei, Zhou, & Mei, 2015) for the synthesis of self-healing carboxymethyl cellulose hydrogels. Briefly, NaCMC was poured in water (cellulose content of 10 or 20% wt.). Due to the high viscosity of NaCMC, this step of pouring and mixing was done first with the help of a high speeded magnet mixer and later, as the viscosity increased, manually with a glass rod. As a result, extremely viscous pastes were obtained (Figure 1a). Hence, to further process these NaCMC pastes, small pieces of rectangular shape

($2.0 \times 1.0 \times 0.1$ cm^3) were prepared with a hydraulic press (10 Pa, 1 min) and were kept at 4 °C prior cross-linking for the formation of hydrogel (Figure 1a). Additionally, 0.5, 1 or 2 M of a supporting electrolytic salt (*i.e.* NaCl, KCl, CaCl, Na_2HPO_4, Na_2SO_4, or $LiClO_4$) and 0.5 M NaN_3, which is a biocide preventing bacterial and fungi growth (0.1 mg/mL), were included in the NaCMC pastes.

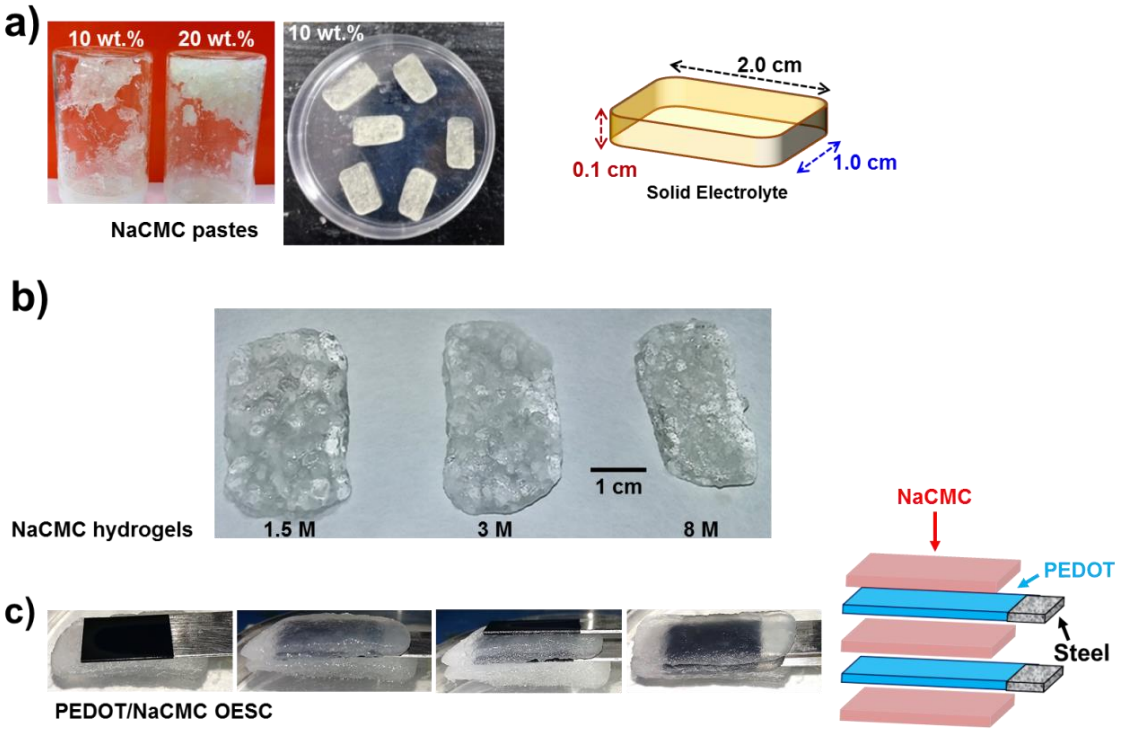

Figure 1. (a) Pieces obtained after molding the NaCMC pastes (10 or 20% wt. cellulose) with a hydraulic press. The dimensions of the pieces are displayed at the right. (b) NaCMC hydrogels cross-linked using acid citric solutions at different concentrations (1.5, 3 or 8 M). (c) Photographs displaying the assembly of the different elements of the PEDOT/NaCMC ESCs. A scheme of the supercapacitor is displayed at the right.

NaCMC polymeric chains were cross-linked by immersing the pieces into 1.5, 3.0 or 8.0 M citric acid solutions for 24 hours at room temperature and slight shaking (80 rpm) (Figure 1b). Scheme 1b depicts the cross-linking achieved. Finally, the excess of citric acid was removed by washing the pieces in distillated water for 48 hours at room

temperature (water was changed every *ca.* 12 hours). After washing, some samples were directly submitted to a reabsorption process of the supporting electrolytic salt (24 hours), whereas others were lyophilized prior such reabsorption. Accordingly, different hydrogel-based SSE configurations were prepared by varying the following three parameters: *i)* the NaCMC paste (with 10 or 20% wt. cellulose and a given concentration of the selected supporting electrolyte); *ii)* the citric acid concentration (1.5, 3.0 or 8.0 M); *iii)* the post-washing treatment (reabsorption of supporting electrolytic salt without or with lyophilization).

Characterization

Optical profilometry. In order to determine the thickness of PEDOT electrodes, several scratches (minimum 4) were intentionally made throughout the surface of the polymer samples (n=6), and the step at several positions along the scratches was measured using a surface profilometer Dektak 150 (Veeco). Data analysis was performed with the computer software Dektatk (version 9.2, Veeco Instruments Inc.).

Electrical conductivity. After partial coating the surface of PEDOT with silver paint to yield two electrodes, the electrical conductivity of the electrodes was assessed by two-probe conductivity measurements.

The conductivity of the hydrogels was determined by electrochemical impedance spectroscopy (EIS). EIS measurements were performed at open circuit (OCP) over the frequency range of 100 kHz to 10 mHz with a potential amplitude of 0.05 V using an AUTOLAB-302N potentiostat/galvanostat. A cell with a geometry explicitly constructed for the analysis of solid polymeric systems like those studied in this work was used in all cases (Müller et al., 2014).

Scanning electron microscopy (SEM). The morphology of NaCMC pastes and hydrogels was observed by SEM using a Focused Ion Beam Zeiss Neon40 scanning electron microscope equipped with an energy dispersive X-ray (EDX) spectroscopy system and operating at 5 kV. All samples were sputter-coated with a thin carbon layer using a K950X Turbo Evaporator to prevent electron charging problems. Prior to SEM observation, samples were lyophilized (*i.e.* freeze-drying). The size of pores was determined from the SEM images using the software SmartTIFF (*v*1.0.1.2.), and data was fitted to a normal curve (OrginPro 8 SR0, v8.0724).

Surface area. The surface area was determined through the Brunauer-Emmet-Teller (BET) method by determined the adsorption of nitrogen using an ASAP 2010 (Accelerated Surface Area and Porosimetry Analyzer, Micromeritics).

Preparation of PEDOT/NaCMC ESCs

NaCMC pastes and biohydrogels, which were used as SSE, were prepared 24 hours before testing. In combination with PEDOT electrodes, the assembly of the supercapacitor device was done in a two-step process. Firstly, NaCMC electrolyte pieces of rectangular shape were obtained as previously described. Secondly, a sandwiched configuration was adopted where NaCMC electrolyte pieces were arranged separating two PEDOT electrodes at a distance of 0.1 cm, as illustrated in Figure 1c. Finally, the external side of each PEDOT electrode was coated with another NaCMC electrolyte piece. On the other hand, a supercapacitor configuration in which the NaCMC-based SSE was replaced by a 0.5 M NaCl aqueous solution was used as control.

Electrochemical characterization

The electrochemical response of PEDOT electrodes was studied in a two-electrode configuration by means of galvanostatic charge/discharge (GCD) and cyclic voltammetry (CV) measurements.

The specific capacitance (*SC*; in F/g) is the capacitance per unit of mass for one electrode, and can be expressed as:

$$SC = 4 \times \frac{C}{m} \quad (1)$$

where *C* is the measured capacitance for the two-electrode cell and *m* the total mass of the active material in both electrodes. The multiplier 4 adjusts the capacitance of the cell and the combined mass of the two electrodes to the capacitance and mass of a single electrode.

GCD is the most commonly used procedure to determine the cell capacitance (*C*; in F) of a pseudocapacitor:

$$C = I \Big/ \left(\frac{dV}{dt}\right) \quad (2)$$

where *I* is the discharging current applied to the device and *dV/dt* should be calculated as $(V_{max} - ½V_{max})/(t_2 - t_1)$, where V_{max} corresponds to the highest voltage in the GCD curve after the voltage drop (V_{drop}) at the beginning of the discharging process.

During the optimization of the NaCMC-based SSE, GCD curves (5 cycles) between 0.0 and 0.8 V were run at different current densities (*i.e.* charge and discharge rates are specified in units of current per electrode mass): 0.30, 0.43, 0.61, 1.22, 2.43 and 5.21 A/g, which corresponded to 0.35, 0.5, 0.7, 1.4, 2.8 and 6 mA, respectively. Besides, the coulombic efficiency (η, %) was evaluated as the ratio between the discharging and charging times (t_d and t_c, respectively) for the electrochemical window between 0.0 V and 0.8 V:

$$\eta = t_d \Big/ t_c \quad (3)$$

Furthermore, CV measurements can also be used to determine the cell capacitance, *C*, by applying Eqn 2. In this case, *I* corresponds to the average current during discharging (*i.e.* PEDOT reduction from 0.8 to 0.0 V), while *dV/dt* is the scan rate. Specifically, cyclic voltammograms (5 cycles) were recorded from 0.0 V (initial and final potentials) to 0.8 V (reversal potential) at different scan rates: 10, 25, 50, 75, 100, 150 and 200 mV/s.

On the other hand, the cycling stability of the selected ESCs was tested by submitting the system to: *(i)* 1400 GCD cycles at a current density of 1.22 A/g from 0.0 V to 0.8 V, which corresponds to t_c and t_d of approximately 40-60 seconds; and *(ii)* 200 CV cycles at a scan rate of 50 mV/s from 0.0 V (initial and final potential) to 0.8 V (reversal potential). This potential interval was found to provide the highest capacitive response of PEDOT electrodes in devices with biopolymeric hydrogels as electrolytes (Pérez-Madrigal et al., 2016a). Moreover, the evaluation of the self-discharging (SD) and leakage current (LC) curves of PEDOT/NaCMC ESCs was carried out applying the following methodologies. In the first case, PEDOT/NaCMC devices were charged to 0.8 V at 0.25 mA and kept at $1 \cdot 10^{-11}$ mA for 10 min (*i.e.* self-discharging). After that time, the device was discharged to 0 V at –1 mA. In the second case, after charging the device to 0.8 V at 0.25 mA, it was kept at 0.8 V for 300-600 seconds while recording the current data through the ESC (*i.e.* leakage current). Data were obtained from testing four different devices.

RESULTS AND DISCUSSION

Preparation of PEDOT electrodes

The novelty presented in this work is based on using NaCMC pastes and hydrogels as aqueous-based SSE for ESCs. Thus, taking into account previous works, PEDOT

electrodes were prepared by a straightforward method (Pérez-Madrigal et al., 2016a; Pérez-Madrigal et al., 2017). Specifically, chronoamperometry was conducted at 1.25 V with a polymerization charge of 500 mC/cm^2. Under these electrochemical conditions, PEDOT films exhibited a thickness of 4.12 ± 0.83 μm, an electrical conductivity of 33.2 ± 4.1 S/cm, and a mass of 1.143 ± 0.097 mg. Spectroscopic and morphological characterization of PEDOT films has been already reported (Pérez-Madrigal et al., 2016a; Pérez-Madrigal et al., 2017).

Preparation and characterization of NaCMC pastes and hydrogels as SSE

Table 1 summarizes the different NaCMC-based systems prepared by adapting the procedure described by Jiang et al. (2015) that uses citric acid as cross-linker (Scheme 1). Although other compounds, such as poly(ethylene glycol) maleate citrate (Gyawali et al., 2010) and alginate/polyvinyl alcohol nanofibers (Stone, Gosavi, Athauda, & Ozer, 2013), have been also used to cross-link cellulose derivatives, citric acid was chosen because of its simplicity, its natural origin, its participation in metabolic routes and the self-healing (Jiang et al., 2015) and superabsorbent (Demitri et al., 2008) properties of the resulting hydrogels.

Figure 1b shows a representative example of washed NaCMC hydrogels obtained after cross-linking the cellulose paste (10% wt.) with 1.5, 3 and 8 M citric acid solutions, hereafter denoted NaCMC-10/1.5, -10/3, and -10/8, respectively. FTIR spectra of the NaCMC hydrogels (Figure S1) show a strong absorption band at ~1600 cm^{-1}, which is characteristic of cellulose, and the peak at ~1730 cm^{-1} of the ester bond that indicates the citric acid reacted with cellulose forming the cross-links (Demitri et al., 2008).

Table 1. List of NaCMC-based SSE systems prepared in this work: optimized parameters and the *SC* (F/g) values obtained from electrochemical testing.

	[NaCMC]	**[Citric acid]**	**Post-washing treatment to recover NaCl**	***SC* (F/g)**	
				CV (50 mV/s)	GCD (1.22 A/g)
0.5 M NaCl [a]	-	-	-	74.6	78.1
NaCMC paste [b]	10% wt.	-	-	58.3 ± 16.3	69.4 ± 16.9
NaCMC paste [b]	20% wt.	-	-	61.5	68.0
NaCMC-10/1.5 [c]	10% wt.	1.5 M	-	-	-
NaCMC-10/3 [c]	10% wt.	3 M	-	-	-
NaCMC-10/8 [c]	10% wt.	8 M	-	-	-
NaCMC-20/8 [c]	20% wt.	8 M	-	-	-
NaCMC-10/1.5/DR	10% wt.	1.5 M	Direct re-absorption by immersion	65.3±4.0	72.9±1.1
NaCMC-10/3/DR	10% wt.	3 M	Direct re-absorption by immersion	58.6	66.1
NaCMC-10/8/DR	10% wt.	8 M	Direct re-absorption by immersion	41.8	46.2
NaCMC-10/1.5/LR	10% wt.	1.5 M	Lyophilization + re-absorption by immersion	59.4	60.7
NaCMC-10/3/LR	10% wt.	3 M	Lyophilization + re-absorption by immersion	60.1	69.4
NaCMC-10/1.5/LR	10% wt.	1.5 M	Lyophilization + re-absorption by immersion	43.9	24.9

[a] Liquid electrolyte used as control. [b] NaCMC-based SSE not cross-linked but containing 0.5 M NaCl. [c] Only prepared for morphological characterization by SEM

All systems display adequate robustness and mechanical stability, which ensure their handling during the assembly of the supercapacitor device (Figure 1c). For the lower citric acid concentrations (1.5 and 3 M), NaCMC paste pieces experienced an increase in volume after the cross-linking/washing steps, this fact being less pronounced for the highest concentration (8 M). Taking this observation into consideration, the swelling ratio (SR, %), which is a good indicative of their cross-linking degree and their moisture content, was determined for NaCMC hydrogels obtained using 10% wt. The SR was defined as:

$$SR = \frac{w_w - w_d}{w_d} \quad (4)$$

where w_w is the weight of the hydrogel after being immersed in distillate water for 24 hours and w_d is the weight of the dried hydrogel (*i.e.* after freeze-drying). NaCMC-10/1.5 and NaCMC-10/3 hydrogels display the higher SR values (SR= 2420% ± 272% and 2205% ± 104%, respectively), while the opposite occurs for NaCMC-10/8 (SR= 1064% ± 149%). These significant differences reflect the remarkable influence of the citric acid concentration in the cross-linking density. Furthermore, the water-content decreases with increasing citric acid concentration.

Figure 2 displays the morphology of NaCMC paste prepared using 10% wt. cellulose and of NaCMC-10/1.5, -10/3, and -10/8 hydrogels subsequently obtained. All systems presented an open structure with abundant pores, which are required to maximize the pseudocapacitance of PEDOT electrodes. Hence, such opened structures promote the ion movement at the electrode-electrolyte interface during charge-discharge processes. The paste, which is not cross-linked, contains 0.5 M NaCl that is covering all the surface of the NaCMC walls (Figures 2a-b). This system presented the most compact structure since the salt is blocking the channels. In contrast, NaCMC-based hydrogels (Figures 2c-f) exhibit cavities with sizes that varied depending on the citric acid

concentration used during the cross-linking step (Figure 2). Specifically, the averaged pore size of NaCMC-10/1.5, -10/3, and -10/8 hydrogels is 41.5 ± 13.1 μm, 58.4 ± 22.3 μm, and 77.9 ± 36.2 μm, respectively, while the BET surface area is 300, 347 and 455 m^2/g, respectively. These results evidence that, although the morphology depends on the cross-linking density, all hydrogels prepared using 10% wt. cellulose present highly open porous structures with well interconnected pores, which are expected to allow an agile migration of the ions under the applied voltage.

The ionic conductivity (σ) of the prepared hydrogels was calculated from the measured bulk resistance (R_b) values obtained in EIS by using the following relation:

$$\sigma = \frac{L}{R_b A} \qquad (4)$$

where L is the distance between two electrodes and A is the active area, which is taken as 1 cm^2. In all cases, Nyquist plots showed the typical shape with a semicircle at high frequencies followed by an inclined spike at low frequencies (Armelin et al., 2016). The reduction of the semicircle was related to the increment of the number of charge carriers and its ionic mobility. Considering that R_b corresponds to the diameter of the semicircle, the σ value decreased from ~10^{-4} S/cm for NaCMC-10/1.5 to ~10^{-6} S/cm for NaCMC-10/8. Thus, the conductivity increases with the decreasing concentration of cross-linkers, indicating that free (*i.e.* not crosslinked) carboxylate groups play a crucial role in the ionic mobility. On the other hand, the σ value increased to 0.014 S/cm after post-washing treatment of NaCMC-10/1.5 hydrogel by reabsorption of 0.5 M NaCl electrolytic salt.

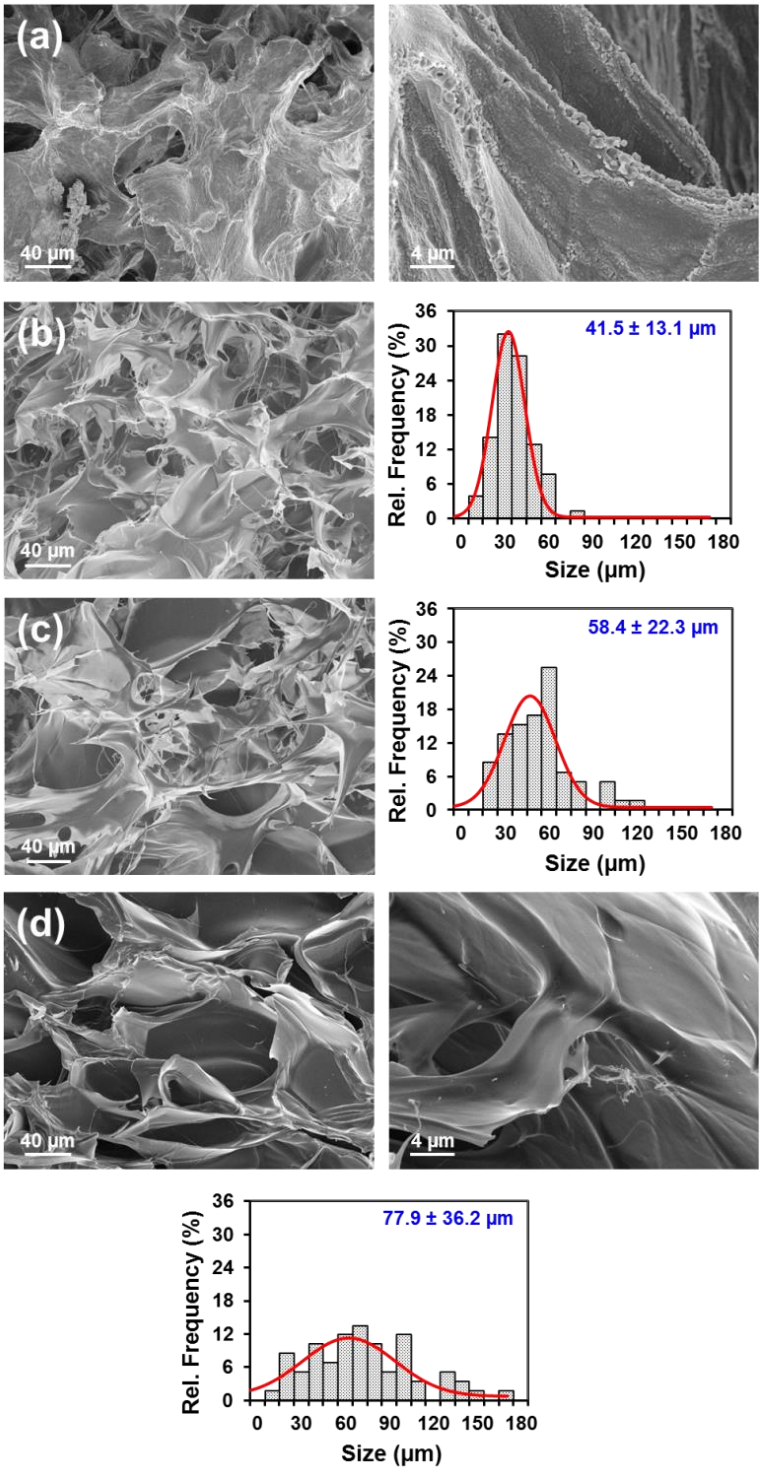

Figure 2. SEM micrographs of (a) NaCMC paste obtained using 10% wt. cellulose and (b) NaCMC-10/1.5, (c) -10/3 and (d) -10/8 hydrogels. The pore size distribution for the three NaCMC-based hydrogels is also displayed.

The morphology of the NaCMC paste obtained with 20% wt. cellulose and the hydrogel obtained using an 8 M citric acid solution, hereafter NaCMC-20/8, are

displayed in Figure S2. Due to the very granular texture of the NaCMC paste with 20% wt. cellulose (Figure 1a), which affects negatively its performance as SSE (discussed in next section), only the biohydrogel cross-linked with the highest concentration of citric acid was prepared. High and low magnification SEM micrographs reveal that the morphology of NaCMC-20/8 resembles those of NaCMC-10/3 and, especially, NaCMC-10/8, with well-defined pores of size 70.5 ± 27.9 μm. Nevertheless, the NaCMC-20/8 walls are significantly thicker in comparison to NaCMC-10/8 due to the higher concentration of NaCMC used to prepare the paste, thus reducing the porosity of the system. This less developed moist pore network was expected to affect negatively the ionic conduction in the electrolyte (Liu, Wu, Wang, & Wang, 2014), as it has been confirmed in next section.

Optimization of the NaCMC-based SSE: SC evaluation

PEDOT's capacitive response is expected to be largely influenced by the characteristics of the SSE. In this section, five main factors have been analysed to optimize the NaCMC-based SSE: *i)* the chemical nature of the inorganic salt used as supporting electrolyte; *ii)* the concentration of such inorganic salt; *iii)* the concentration of cellulose used to prepare the paste; *iv)* the concentration of citric acid employed during cellulose cross-linking; and *v)* the treatment applied to recover the inorganic supporting electrolyte after washing.

In this section, electrochemical characterizations have been conducted using CV and GCD. It should be noted that the potential intervals used in such characterizations are limited by the electrochemical splitting of water molecules (water hydrolysis) contained in NaCMC-based pastes and hydrogels. Indeed, we fixed this as the optimum one in previous studies on hydrogels (Pérez-Madrigal et al., 2016a, 2017). Moreover, in this

work the utilization of cellulose-based electrolytic systems has been combined with green chemistry approaches. Therefore, the use of organic solvents for the fabrication of cellulose organogels, which could allow the increase of the potential interval, has not been considered.

Selection of the inorganic salt as supporting electrolyte. Figures 3a compares the cyclic voltamograms (5^{th} cycle) of the NaCMC paste obtained using 10% wt. cellulose and containing different inorganic salts as supporting electrolyte: NaCl, KCl, $CaCl_2$, $LiClO_4$, Na_2SO_4 or Na_2HPO_4. As it can be seen, the supercapacitive response of PEDOT electrodes is remarkably influenced by the chemical characteristics of the salt. In particular, ESCs containing NaCl, KCl and $CaCl_2$ exhibit better capacitive behavior than those with $LiClO_4$, Na_2SO_4 and Na_2HPO_4 within the potential window from 0.0 V to +0.8 V at a scan rate of 50 mV/s, as it is evidenced by the higher areas and the near rectangular shape of the voltammetric curves. This has been correlated with the size of the ions. Thus, the effective reaching of the ions to the electrode-electrolyte interface improves with their decreasing size. Similar conclusions are derived from the galvanostatic charge-discharge (GCD) curves displayed in Figure 3b. Although symmetric GCD curves with a typical triangular shape and a V_{drop} at the beginning of the discharging were obtained in all cases, the higher discharging times were achieved for NaCl and KCl.

Figures 3c and 3d represent the variation of the *SC* (Eqn 1) against the scan rate and the current density, respectively, as determined from CV and GCD capacitances (Eqn 2) for the different supporting electrolytes. As it can be seen, the highest *SC* values were obtained for NaCl, independently of both the scan rate and current density, even though the values achieved with KCl and $CaCl_2$ were pretty close. On the other hand, the *SC*

values derived from the 2nd and 5th GCD cycles were practically identical in all cases, evidencing the stability of the PEDOT response. On the basis of these results and considering that NaCl is non-toxic, abundant, and very cheap, it was chosen as the most appropriated supporting electrolyte to be combined with NaCMC-based pastes and hydrogels, resulting in sustainable green SSEs.

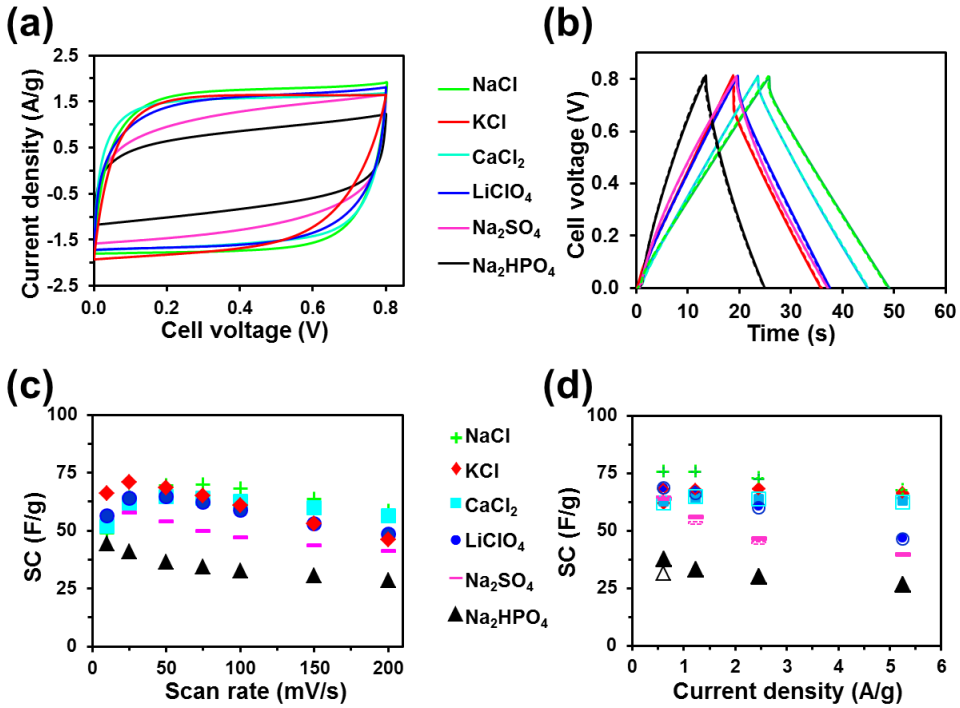

Figure 3. Supercapacitor response of PEDOT/NaCMC ESCs in which the SSE was prepared using NaCMC paste with 10% wt. cellulose and different inorganic salts (0.5 M) as supporting electrolyte: (a) 5th cyclic voltammogram recorded at 50 mV/s; (b) 2nd (solid line) and 5th (dashed line) GCD curves recorded at 1.22 A/g; (c) *SC* values obtained from CV measurements at different scan rates; and (d) *SC* values derived from the 2nd (filled symbols) and the 5th (empty symbols) GCD curves at several current densities.

Selection of the NaCl concentration. Potentiostatic and galvanostatic electrochemical assays similar to those displayed in Figures 3 were performed considering 0.5, 1 and 2 M NaCl as supporting electrolyte for the NaCMC paste with 10% wt. cellulose SSE. Results, which are displayed in Figure 4, were compared with those obtained for a

supercapacitor configuration in which PEDOT electrodes were immersed in a 0.5 M aqueous NaCl solution.

The capacitive response was better for the SSE-containing ESC devices than for those with the liquid control electrolyte. Indeed, ESCs with the latter configuration experienced a loss of rectangular shape in the cyclic voltammogram (Figure 4a) and an increment of V_{drop} in the GCD curve (Figure 4b). On the other hand, the influence of the NaCl concentration as supporting electrolyte of NaCMC-based SSEs is very small. Thus, cyclic voltammograms, GCD curves, and *SC* values obtained for ESCs with different salt concentration in the SSE are almost superimposable. From these results, the concentration of NaCl as supporting electrolyte was kept at 0.5 M.

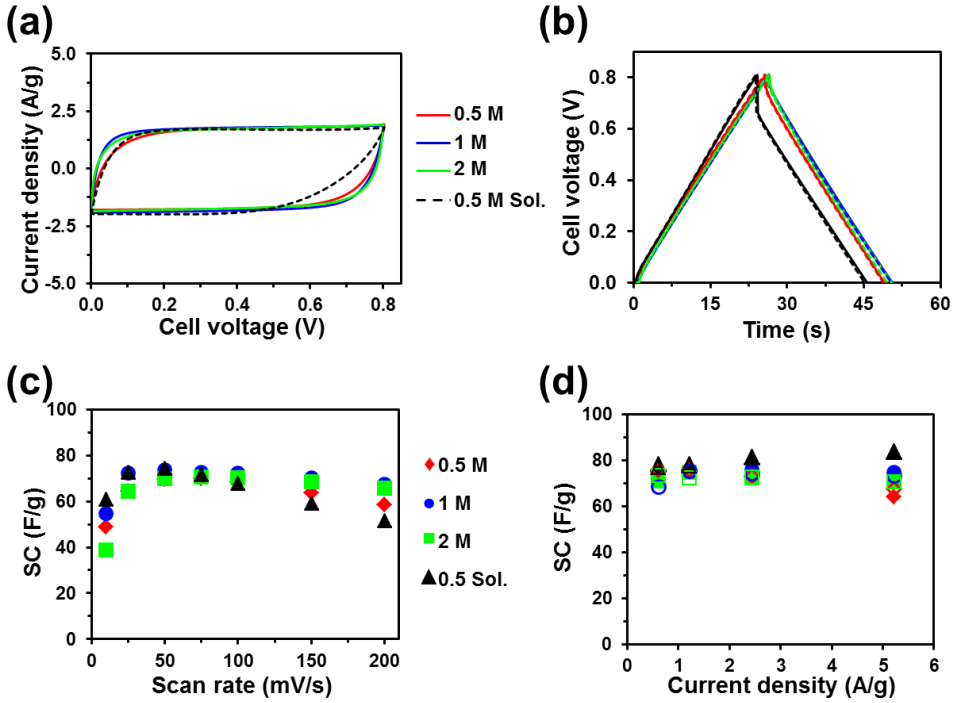

Figure 4. Supercapacitor response of PEDOT/NaCMC ESCs in which the SSE was prepared using NaCMC paste with 10% wt. cellulose and different NaCl concentrations (0.5, 1 and 2 M) as supporting electrolyte: (a) 5th cyclic voltammogram recorded at 50 mV/s; (b) 2nd (solid line) and 5th (dashed line) GCD curve recorded at 1.22 A/g; (c) *SC* values obtained from CV measurements at different scan rates; and (d) *SC* values derived from the 2nd (filled symbols) and the 5th (empty symbols) GCD curves at several

current densities. The response of PEDOT in 0.5 M aqueous NaCl solution (control) is also displayed.

Concentration of cellulose. Figure 5 compares the response of PEDOT electrodes when NaCMC pastes made with 10% wt. and 20% wt. cellulose, in both cases containing 0.5 M NaCl as supporting electrolyte, are used as SSE. The potentiostatic and galvanostatic responses are slightly better for the system with 10% wt. cellulose than for the one with 20% wt. For example, GCD curves for the latter deviate from the ideal triangular shape, while the shape of the voltage change with increasing time corresponds to a nearly perfect triangle for the ESC with the 10% wt. NaMCM paste. Also, the V_{drop} is more pronounced in the supercapacitor with the highest concentration of cellulose. As a consequence of such differences, the *SC* of the ESC with the lowest concentration of cellulose paste in the SSE is the highest, independently of both the scan rate and current density. These results have been attributed to the internal viscosity of the SSE, which grows with the concentration of the cellulose. More specifically, the amount of water inside the paste decreases with increasing concentration of cellulose, hindering the movement of ions across the interconnected porous network (Liu et al., 2014). Hence, hereafter all ESCs are prepared using SSEs with 10% wt. NaCMC.

Concentration of citric acid and post-washing treatment. NaCMC-10/1.5, NaCMC-10/3 and NaCMC-10/8 hydrogels were prepared immersing the NaCMC paste obtained using 10% wt. cellulose and 0.5 M NaCl into 1.5, 3 and 8 M citric acid solutions, respectively. After the cross-linking, hydrogels were washed to eliminate the excess of citric acid. However, the concentration of NaCl introduced as supporting electrolyte into the paste decreased during such washing step, which was evidenced by the very low *SC* values obtained when washed hydrogels were used as SSE (not shown). In an effort to

overcome this problem, two post-washing treatments are proposed in this work to recover the concentration of supporting electrolyte. The first one is based on the immersion of the samples in a NaCl solution (0.5 M) for 24 hours just after the washing step (*i.e.* direct NaCl re-absorption), hydrogels obtained using this strategy being denoted NaCMC-10/#/DR (where # corresponds to the concentration of citric acid in the cross-linking step). In the second approach, hydrogels are lyophilized between the washing and the reabsorption processes. Hereafter, hydrogels obtained by applying such lyophilization intermediate step are denoted NaCMC-10/#/LR.

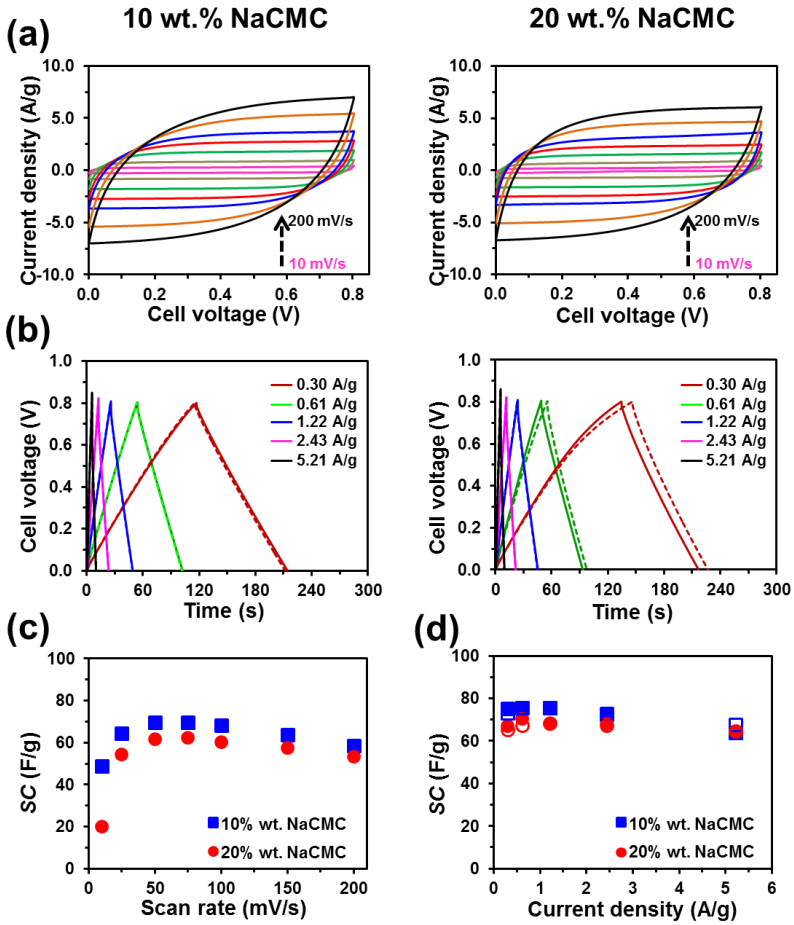

Figure 5. Supercapacitor response of PEDOT/NaCMC ESCs obtained using NaCMC paste with 10% wt. and 20% wt. cellulose (left and right, respectively) and 0.5 M of NaCl as supporting electrolyte: (a) 5th cyclic voltammogram recorded at different scan rates (10, 25, 50, 75, 100, 150, and 200 mV/s); and (b) 2nd (solid line) and 5th (dashed line) GCD curves at different current densities (0.30, 0.61, 1.22, 2.43 and 5.21

A/g). (c) *SC* values obtained from the cyclic voltammograms displayed in (a). (d) *SC* values obtained from the 2nd (filled symbols) and the 5th (empty symbols) GCD curves displayed in (b).

Cyclic voltammograms and GCD curves recorded for ESCs constructed using PEDOT electrodes and NaCMC-10/#/DR and NaCMC-10/#/LR SSE are displayed in Figures S1 and S2, respectively, while the variation of the *SC* against the scan rate and the current density are compared in Figures 6a and 6b, respectively. As it can be seen, the potentiostatic and galvanostatic *SC*s are slightly higher for NaCMC-10/#/DR than for NaCMC-10/#/LR for hydrogels obtained using 1.5 and 8 M citric acid, while the influence of the post-washing treatment on hydrogels cross-linked in a 3 M citric acid solution depends on both the scan rate and the current density. Thus, *SC* values are higher for NaCMC-10/3/DR than for NaCMC-10/3/LR, or at least similar, when CV and GCD assays were conducted at low scan rates (10 and 25 mV/s) and current densities (< 1.5 A/g), respectively. However, in general, the best capacitive behavior is obtained with the NaCMC-10/1.5/DR SSE, which shows a behavior similar to the control NaCl electrolytic solution.

The coulombic efficiency (η), which is defined as the ratio of discharging time and charging time when the charge–discharge current densities are equal (Eqn 3), was calculated for evaluating the influence of the hydrogel structure and the post-washing treatment on the charge transfer efficiency. Results obtained for NaCMC-10/#/DR and for NaCMC-10/#/LR, which are compared in Figure 6c, indicate that the highest charge transfer efficiency was obtained for the NaCMC-10/1.5/DR SSE, η values achieved for the latter being slightly higher than those achieved for the control NaCl electrolytic solution.

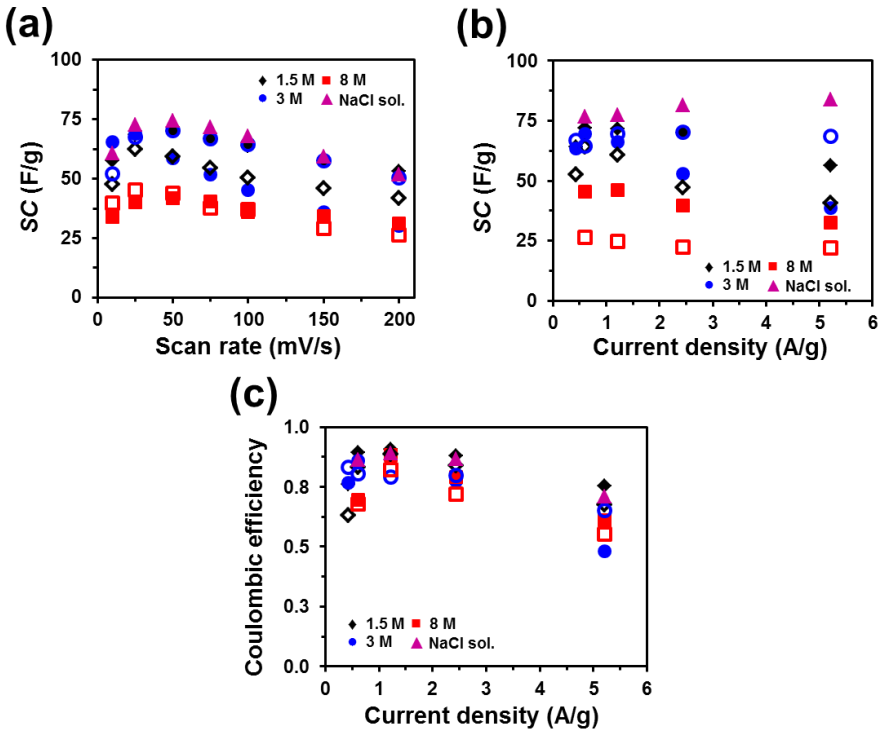

Figure 6. Supercapacitor response of the PEDOT/NaCMC ESCs with NaCMC-10/1.5, NaCMC-10/3 and NaCMC-10/8 hydrogels as SSE: (a,b) *SC* values obtained from the (a) cyclic voltammograms and (b) GCD curves displayed in Figures S2 and S3, respectively; (c) Coulombic efficiency derived from the GCD curves displayed in Figures S2 and S3. (a-c) Filled symbols correspond to hydrogels that were submitted to a direct re-absorption process (NaCMC-10/#/DR; Figure S3), while empty symbols refer to hydrogels that were lyophilized prior such reabsorption (NaCMC-10/#/LR; Figure S4).

Overall, after examining the effects of the chemical nature and concentration of the salt used as supporting electrolyte, the amount of cellulose in the paste, the concentration of citric acid used for cross-linking and the post-washing treatment in the *SC*, the better PEDOT capacitance responses have been identified for the NaCMC paste obtained using 10% wt. cellulose and 0.5 M NaCl as supporting electrolyte (NaCMC-10 paste) and the hydrogel achieved by cross-linking such paste into a 1.5 M citric acid solution and applying a direct NaCl reabsorption treatment after the washing step

(NaCMC-10/1.5/DR). In consequence, such two SSEs have been further characterized in the next section.

Supercapacitor device with optimized NaCMC-based SSE

The response of symmetric ESCs constructed using two PEDOT electrodes and NaCMC paste prepared with 10% wt. cellulose and 0.5 M NaCl or NaCMC-10/1.5/DR hydrogel as SSE, has been evaluated in this section. More specifically, the *SC*, cyclability, self-discharging (SD) and leakage-current (LC) responses of such devices, hereafter denoted PEDOT/NaCMC-10(paste) and PEDOT/NaCMC-10/1.5/DR ESCs, respectively, have been evaluated in triplicate and compared with that achieved for analogous symmetric supercapacitor in which the SSE is replaced by a 0.5 M NaCl aqueous solution. It is worth noting that, although aqueous-based electrolytic systems (*e.g.* NaCl, KOH, H_2SO_4 and Na_2SO_4 solutions) have been extensively used because of their good response, SSEs are attracting increasing attention since they present important advantageous characteristics: flexibility, light-weight, easy of handling, elimination of liquid leaking and enhancement of the device compactness.

The capacitive behavior of the selected ESCs, as determined by means of CV and GCD, is compared in Figure S5. From CVs, it can be observed that whereas PEDOT/ NaCMC-10/1.5/DR performs better at low scan rates, the *SC* of PEDOT/NaCMC–10(paste) is higher when the scan rate is > 100 mV/s (Figure S5a). GCDs assays show that the behavior is better for PEDOT/ NaCMC-10/1.5/DR than for PEDOT/NaCMC-10(paste) at all current densities, especially at high ones (Figure S5b). These results indicate that the capacitive performance of the devices is good, existing a non-high contact resistance between the PEDOT electrodes and the two selected NaCMC-based SSEs. Consequently, the *SC* and coulombic efficiency (Figure S5c) values obtained for

PEDOT/NaCMC-10(paste) and PEDOT/NaCMC-10/1.5/DR ESCs are in the same order of magnitude than those obtained for the control device (Figures S5a-b) except at high current densities (*i.e.* >5 A/g) where the performance of the devices containing NaCMC is manifestly lower.

The cyclability of PEDOT/NaCMC-10(paste) and PEDOT/NaCMC-10/1.5/DR was evaluated by both CV (200 cycles) and GCD (1400 cycles), results being compared in Figures 7a and 7b, respectively. The behavior exhibited by PEDOT/NaCMC-10(paste) is similar to that typically obtained for ESCs, the area of voltammogram and the charge-discharge times decreasing with the number of cycles. The *SC* retention after 200 redox cycles and 1400 charge-discharge cycles at room temperature was of 86% and 61%, respectively. Amazingly, PEDOT/NaCMC-10/1.5/DR behaves very differently, the area of the voltammogram and the charge-discharge times increasing with the number of cycles. Thus, the *SC* of this ESC increased by 6% and 15% after 200 redox cycles and 1400 charge-discharge cycles at room temperature, respectively. This may be attributed to two different reasons: (1) the increment of the concentration of ions accessing and escaping from the PEDOT electrodes due occurrence of some type of catalytic reaction in the cell; or (2) the reduction of the porosity of the electrode material due to some structural changes that enhance the access and escape of dopant ions. In any case, according to these electrochemical observations, the PEDOT/ NaCMC-10/1.5/DR ESC should be considered as self-electrostabilized.

Another parameter obtained from the charge curves (Figure 7b) is the RC time constant ($\tau=RC$), which indicates the time interval over which voltage, charge, and current change in a circuit. More specifically, τ is the time required to charge a capacitor, through a resistor, from an initial voltage of zero to *ca.* 63.2% of the value of an applied DC voltage (in our case 0.51 V). Hence, the time constant (in seconds) for

the PEDOT/NaCMC-10(paste) and PEDOT/NaCMC-10/1.5/DR systems are 27.6/20.8 and 24.9/28.3 for the 2nd/1400th cycle, respectively (Figure S6). Interestingly, the RC time constant displayed by the PEDOT/NaCMC-10/1.5/DR device is slightly higher after 1400 charge-discharge cycles, whereas it decreases considerably for the PEDOT/NaCMC-10(paste) system, which is charged and discharged faster with the number of consecutive cycles. Indeed, these results show the robustness of the PEDOT/NaCMC-10/1.5/DR device, which displays a performance less affected by the number of charging cycles.

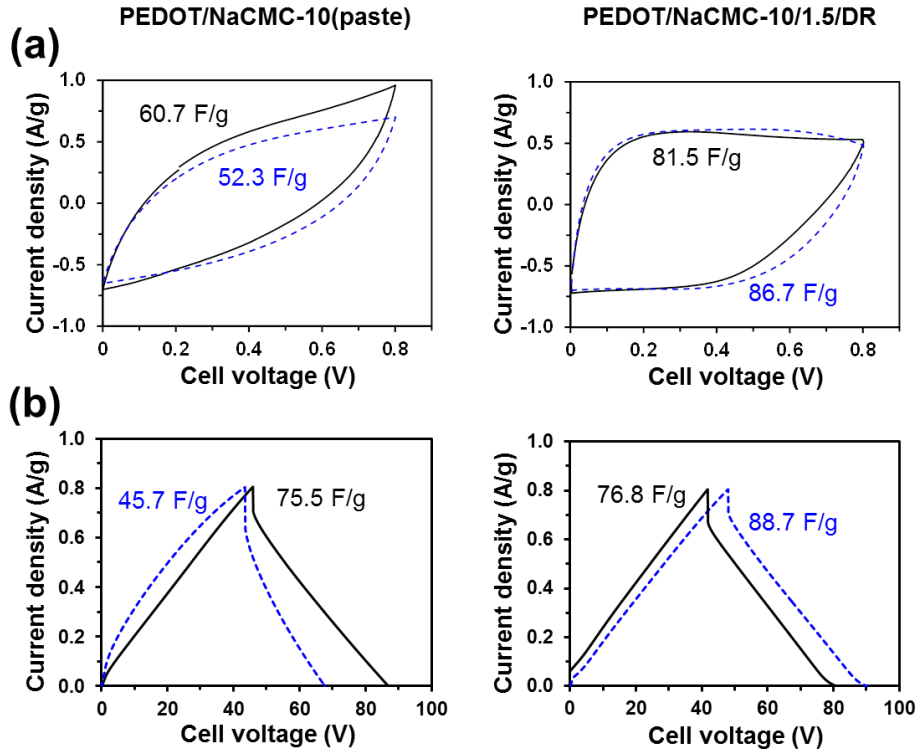

Figure 7. Cyclability of PEDOT/NaCMC-10(paste) and PEDOT/NaCMC-10/1.5/DR ESCs: (a) 1st (solid black line) and 200th (blue dashed line) cyclic voltammograms recorded at 25 mV/s; and (b) 2nd (solid black line) and 1400th (dashed blue line) GCD curves recorded at 0.61 A/g.

Self-discharge (SD) is understood as the voltage drop on a charged capacitor after a stipulated period of time. Such losses of charge may result in dysfunctional conditions,

affecting the electrochemical response of the capacitor by lowering the power and energy densities. That is why self-discharge has a major practical significance when assessing the specifications and performance of any energy storage device. For PEDOT/NaCMC-10(paste) and PEDOT/NaCMC-10/1.5/DR ESCs, the SD response was evaluated by keeping the charged device at 1×10^{-11} mA for 10 min (self-discharge) and, after this period of time, the device was discharged to 0.0 V at –1 mA. Four independent devices were considered for each ESC (Figure 8a).

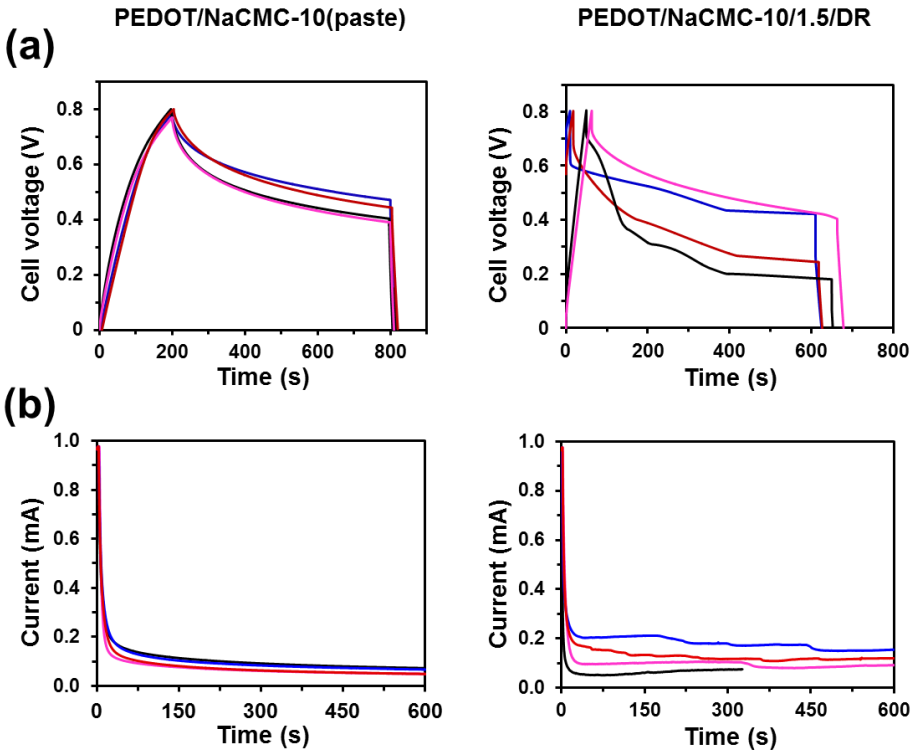

Figure 8. (a) SD response of PEDOT/NaCMC-10(paste) and PEDOT/NaCMC-10/1.5/DR ESCs (n=4) charged to 0.8 V at 0.25 mA and kept at $1\cdot10^{-11}$ mA for 10 min. (b) LC response of PEDOT/NaCMC-10(paste) and PEDOT/NaCMC-10/1.5/DR ESCs (n=4) charged at 0.25 mA and kept at 0.8 and 0.4 V, respectively, for 300-600 s.

PEDOT/NaCMC-10(paste) devices present a homogeneous behavior with final voltages over 0.4 V, indicating a retention >50% in the short term and ensuring specific practical applications. Oppositely, ESCs with the hydrogel-based SSE display a more

disperse behavior with a final voltage comprised between 0.2 and 0.4 V (*i.e.* the average value is 0.34 V, which corresponds to a retention of 42.5%. Self-discharge is influenced by different factors, such as the chemistry and electrochemistry of the system, the purity of reagents and electrolyte, and the temperature (Andreas, 2015). The heterogeneity observed for PEDOT/NaCMC-10/1.5/DR suggests structural and/or compositional inconsistencies in the biohydrogel used as SSE. Although elucidation of the mechanisms and reasons of the disperse behavior observed for PEDOT/NaCMC-10/1.5/DR ESCs is beyond the scope of this study, results suggests that it is probably related to self-electrostabilizing performance observed in the previous cyclability studies (Figure 7).

The leakage current (LC) is the stable parasitic current expected when the capacitor is held indefinitely on charge at the rated voltage. Figure 8b shows the LC response of the two examined ESCs. It has to be taken into account that the voltage maintained for each device differs since PEDOT/NaCMC-10/1.5/DR ESCs were not stable at 0.8 V (Figure S7). Consequently, a more moderated voltage (0.4 V) was chosen for this experiment (Figure 8b, right), and the ESC evidenced an averaged minimum current of 0.1 mA. In contrast, for PEDOT/NaCMC-10(paste), which displays much more standard behavior, the current quickly decreases to a minimum value of 0.0594 mA (Figure 8b, left), staying at that value for the remaining time. This small leakage current is associated with the good stability of ESCs constructed using cellulose-based paste (10% wt.) with NaCl as SSE, which is crucial for energy storage applications.

Cellulose has been successfully used in previous recent works as SSE in ESCs. For example, aerogels made of cellulose nanofibers, which were used as aqueous electrolyte nanoreservoirs, combined with graphene oxide or multi-walled carbon nanotubes electrodes displayed a *SC* of 207 or 178 F/g, respectively (Gao et al., 2013a; Gao et al.,

2013b;). More recently, MnO_2 and reduced graphene oxide nanosheet-piled hydrogel electrodes were combined with bacterial cellulose-filled polyacrylic acid gel electrolyte, a *SC* of 27 F/g being obtained (Fei et al., 2017). In a very recent study (Jiao et al., 2018), a solid electrolyte made of nanofibrillated cellulose combined with polystyrene sulfonic acid, as proton transported polymer, was sandwiched between two paper-based electrodes, the resulting *SC* (81.3 F/g) being comparable to those achieved in this work. However, in all these cases the *SC* values mainly depend on the electrochemical properties of the electrodes, making difficult the comparison among SSEs. In a recent study, we used PEDOT electrodes identical to those reported in this work to evaluate the performance of κ-carrageenan (a linear sulfated polysaccharide that is obtained from red edible seaweeds), sodium alginate (an anionic linear polysaccharide very abundant in nature that is synthesized by brown seaweeds and by soil bacteria) and gelatin (a heterogeneous mixture of water-soluble proteins of high average molecular masses, present in collagen) hydrogels as SSEs (Pérez-Madrigal et al., 2016a). The galvanostatic *SC* determined at 0.6 A/g for ESCs made of κ-carrageenan, sodium alginate and gelatin hydrogels was 78.8, 60.8 and 42.3 F/g, respectively. Accordingly, the performance as SSE of the cellulose paste and the cellulose hydrogel optimized in the present work (*SC* of 75.5 and 76.8 F/g, respectively, in Figure 7b) is comparable to that κ-carrageenan hydrogel and higher than those of sodium alginate and gelatin hydrogels.

CONCLUSIONS

Results obtained in this work indicate that NaCMC is a promising cellulose derivative for preparing SSEs for ESCs. Both pastes and hydrogels, in which NaCMC chains have been cross-linked with citric acid through a simple and straightforward protocol, have been prepared using a salt as supporting electrolyte. The response of the

ESC electrodes depends on both the salt type and salt concentration contained in the NaCMC-based SSE, 0.5 M NaCl being the most suitable electrolytic conditions for PEDOT electrodes. The ESC response also depends on internal characteristics of the hydrogels, NaCMC cross-linked at 1.5 M citric acid exhibiting an adequate performance. Finally, direct re-absorption has been identified as the most suitable post-washing treatment for recovering the concentration of supporting electrolyte in hydrogels, after the washing step.

Electrochemical assays using the optimized PEDOT/NaCMC-10(paste) and PEDOT/NaCMC-10/1.5/DR ESCs prove that the NaCMC paste prepared with 10% wt. cellulose and 0.5 M NaCl and the NaCMC-10/1.5/DR hydrogel exhibit excellent performance when used as SSE. Thus, PEDOT electrodes show high capacitive response and cyclability, as well as low leakage current and self-discharge. Moreover, the NaCMC-10/1.5/DR hydrogel is self-electrostabilizing. Consequently, the *SC* of PEDOT/NaCMC-10/1.5/DR increases with the number of cycles, even though the SD and LC responses are less homogeneous than those displayed by PEDOT/NaCMC-10(paste). In summary, the NaCMC-based architectures facilitate the ion diffusion process and, therefore, are excellent candidates as SSEs for energy storage applications where low cost and lightweight materials from renewable sources are desired.

ACKNOWLEDGEMENTS

Authors acknowledge MINECO/FEDER (MAT2015-69367-R) and the Agència de Gestió d'Ajuts Universitaris i de Recerca (2017SGR359) for financial support. Support for the research of C.A. was received through the prize “ICREA Academia” for excellence in research funded by the Generalitat de Catalunya. Costa Rica National

Commission of Scientific and Technological Research (CONICYT-Support N8FI-172B-14) (to M.C.G.S)

REFERENCES

Andreas, H. A. (2015). Self-discharge in electrochemical capacitors: A perspective article. *Journal of Electrochemical Society, 162*, A5047.

Armelin, E., Pérez-Madrigal, M. M., Alemán, C., & Díaz, D. D. (2016). Current status and challenges of biohydrogels for applications as supercapacitors and secondary batteries. *Journal of Materials Chemistry A, 4*, 8952–8968.

Bao, L., & Li, X. (2012) Towards textile energy storage from cotton t-shirts. *Advanced Materials, 24*, 3246–3252.

Cao, L. J., Yang, M. Y., Wu, D., Lyu, F. C., Sun, Z. F., Zhong, X. W., Pan, H., Liu, H. T., & Lu, Z. G. (2017) Biopolymer-chitosan based supramolecular hydrogels as solid state electrolytes for electrochemical energy storage. *Chemical Communications, 53*, 1615–1618.

Conway, B. E. (1999). Electrochemical supercapacitors.Springer Science+Buisness Media. New York, USA, (Chaper 10, pp. 221–257).

Cui, C., Li, M. Z., Liu, J. Y., Wang, B., Zjang, C., Jiang, L., & Cheng, Q. F. (2014). A strong integrated strength and toughness artificial nacre based on dopamine cross-linked graphene oxide. *ACS Nano, 8*, 9511–9517.

Chen, C., Xu, G., Wei, W., & Yang, L. (2016). A macroscopic three-dimensional tetrapod-separated graphene-like oxygenated N-doped carbon nanosheet architecture for use in supercapacitors. *Journal of Materials Chemistry A, 4*, 9900–9909.

Demitri, C., Del Sole, R., Scalera, F., Sannino, A., Vasapollo, G., Maffezzoli, A., Ambrosio, L., & Nicolais, L. (2008). Novel superabsorbent cellulose-based hydrogels crosslinked with citric acid. *Journal of Applied Polymer Science*, *110*, 2453–2460.

Fei, H., Yang, C., Bao, H., & Wang, G. (2014). Flexible all-solid-state supercapacitors based on graphene/carbon black nanoparticle film electrodes and cross-linked poly(vinyl alcohol)-H_2SO_4 porous gel electrolytes. *Journal of Power Sources*, *266*, 488–495.

Fei, H. J., Saha, N., Kazantseva, N., Moucka, R., Cheng, Q. L., & Saha, P. (2017). A highly flexible supercapacitor based on MnO_2/RGO nanosheets and bacterial cellulose-filled gel electrolyte. *Materials*, *10*, 1251.

Gao, K., Shao, Z., Li, J., Wang, X., Peng, X., Wang, W., & Wang, F. (2013a). Cellulose nanofiber–graphene all solid-state flexible supercapacitors. *Journal of Materials Chemistry A*, *1*, 63–67.

Gao, K., Shao, Z., Wang, X., Zhang, Y., Wang, W., & Wang, F. (2013b). Cellulose nanofibers/multi-walled carbon nanotube nanohybrid aerogel for all-solid-state flexible supercapacitors. *RSC Advances.*, *3*, 15058–15064.

Gao, W., Singh, N., Song, L., Liu, Z., Mohana-Reddy, A. L., Ci, L., Vajtai, R., Zhang, Q., Wei, B., & Ajayan, P. M. (2011). Direct laser writing of micro-supercapacitors on hydrated graphite oxide films. *Nature Nanotechnology*, *6*, 496–500.

Gui, Z., Zhu, H., Gillette, E., Han, X., Rubloff, G. W., Hu, L., & Lee, S. B. (2013). Natural cellulose fiber as substrate for supercapacitor. *ACS Nano*, *7*, 6037–6046.

Guo, H., Yeh, M.-H., Zi, Y., Wen, Z., Chen, J., Liu, G., Hu, C., & Wang, Z. L. (2017). Ultralight cut-paper-based self-charging power unit for self-powered portable electronic and medical systems. *ACS Nano*, *11*, 4475–4482.

Gyawali, D., Nair, P., Zhang, Y., Tran, R. T., Zhang, C., Samchukov, M., Makarov, M., Kim, H. K. W., & Yang, J. (2010). Citric acid-derived in situ crosslinkable biodegradable polymers for cell delivery. *Biomaterials*, *31*, 9092–9105.

Hamedi, M. M., Hajian, A., Fall, A. B., Håkansson, K., Salajkova, M., Lundell, F., Wågberg, L., & Berglund, L. A. (2014). Highly conducting, strong nanocomposites based on nanocellulose-assisted aqueous dispersions of single-wall carbon nanotubes. *ACS Nano*, *8*, 2467–2476.

Håkansson, K. M. O., Henriksson, I. C., de la Peña Vázquez, C., Kuzmenko, V., Markstedt, K., Enoksson, P., & Gatenholm, P. (2016). Solidification of 3D printed nanofibril hydrogels into functional 3D cellulose structures. *Advanced Materials Technologies*, *1*, 1600096.

Hibino, T., Kobayashi, K., Nagao, & Kawasaki, S. (2015). High-temperature supercapacitor with a proton-conducting metal pyrophosphate electrolyte. *Scientific Reports*, *5*, 7903.

Jiang, W., Gao, J., Wei, Z., Zhou, J., & Mei, Y. (2015). Facile fabrication of self-healing carboxymethyl cellulose hydrogels. *European Polymer Journal*, *72*, 514–522.

Jiao, F., Edberg, J., Zhao, D., Puzinas, S., Khan, Z., Makie, P., Naderi, A., Lindstrom, T., Oden, M., Engqist, I., Berggren, M., & Crispin, X. (2018). Nanofibrillated cellulose-based electrolyte and electrode for paper-based supercapacitors. *Advanced Sustainable Systems*, *2*, UNSP 1700121.

Jost, K., Stenger, D., Perez, C. R., McDonough, J. K., Lian, K., Gogotsi, Y., & Dion, G. (2013) Knitted and screen printed carbon-fiber supercapacitors for applications in wearable electronics. *Energy & Environmental Science*, *6*, 2698–2705.

Kühne, R. (2010). Electric buses – an energy efficient urban transportation means. *Energy*, *35*, 4510–4513.

Lee, G., Kang, S. K., Won, S. M., Gutruf, P., Jeong, Y. R., Koo, J., Lee, S. S., Rogers, J. A., & Ha, J. S. (2017). Fully biodegradable microsupercapacitor for power storage in transient electronics. *Advanced Energy Materials*, *7*, 1700157.

Liu, L., Niu, Z., Zhang, L., Zhou, W., Chen, X., & Xie, S. (2014). Nanostructured graphene composite papers for highly flexible and foldable supercapacitors. *Advanced Materials*, *26*, 4855–4862.

Liu, X., Wu, D., Wang, H., & Wang, Q. (2014). Self-recovering tough gel electrolyte with adjustable supercapacitor performance. *Advanced Materials*, *26*, 4370–4375.

Lu, X., Yu, M., Wang, G., Tong, Y., & Li, Y. (2014). Flexible solid-state supercapacitors: design, fabrication and applications. *Energy & Environmental Science*, *7*, 2160–2181.

Mantravadi, R., Chinnam, P. R., Dikin, D. A., & Wunder, S. L. (2016). High conductivity, high strength solid electrolytes formed by in situ encapsulation of ionic liquids in nanofibrillar methyl cellulose networks. *ACS Applied Materials & Interfaces*, *8*, 13426–13436.

Miller, J. R., & Simon, P. (2008). Electrochemical capacitors for energy management, *Science*, *321*, 651–652.

Müller, F., Ferreira, C. A., Azambuja, D., Alemán, C., & Armelin, E. (2014). New sulfonated polystyrene and styrene–ethylene/butylene–styrene block copolymers for applications in electrodialysis. *The Journal of Physical Chemistry B*, *118*, 1102–1112.

Mondal, D., Perween, M., Srivastava, D. N., & Ghosh, P. K. (2014) Unconventional electrode material prepared from coir fiber through sputter coating of gold: A study toward value addition of natural biopolymer. *ACS Sustainable Chemistry & Engineering*, *2*, 348–352.

Nyholm, L., Nyström, G., Mihranyan, A., & Strømme, M. (2011). Toward flexible polymer and paper-based energy storage devices. *Advanced Materials*, *23*, 3751–3769.

Pavković, D., Hoić, M., Deur, J., & Petrić, J. (2014). Energy storage systems sizing study for a high-altitude wind energy application, *Energy*, *76*, 91–103.

Pérez-Madrigal, M. M., Estrany, F., Armelin, E., Díaz-Díaz, D., & Alemán C. (2016a). Towards sustainable solid-State supercapacitors: Electroactive conducting polymers combined with biohydrogels. *Journal of Materials Chemistry A*, *4*, 1792–1805.

Pérez-Madrigal, M. M., Edo, M. G., & Alemán, C. (2016b). Powering the future: application of cellulose-based materials for supercapacitors, *Green Chemistry*, **18**, 5930–5956.

Pérez-Madrigal, M. M., Edo, M., Díaz, A., Puiggalí, J., & Alemán, C. (2017). Poly-γ-glutamic acid hydrogels as electrolyte for poly(3,4-ethylenedioxythiophene)-based supercapacitors. *The Journal of Physical Chemistry C*, *121*, 3182−3193.

Rezzak, D. & Boudjerda, N. (2017). Management and control strategy of a hybrid energy source fuel cell/supercapacitor in electric vehicles. *International Transactions on Electrical Energy Systems*, *27*, e2308.

Saborío, M. C. G., Lanzalaco, S., Fabregat, G., Puiggali, J., Estrany, F. & Aleman, C. (2018) Flexible electrodes for supercapacitors based on the supramolecular assembly of biohydrogel and conducting polymer. *The Journal of Physical Chemistry C*, *122*, 1078–1090.

Stone, S. A., Gosavi, P., Athauda, T. J., & Ozer, R. R. (2013). In situ citric acid crosslinking of alginate/polyvinyl alcohol electrospun nanofibers. *Mater. Lett.*, *112*, 32–35.

Sudhakar, Y. N., Bhat, D. K., Selvakumar, M. (2016). Ionic conductivity and dielectric studies of acid doped cellulose acetate propionate solid electrolyte for supercapacitor. *Polymer Engineering & Science*, *56*, 196–203.

Wang, X. D., Yao, C. H., Wang, F., & Li, Z. D. (2017). Cellulose-based nanomaterials for energy applications. *Small*, *13*, 1702240.

Wang, Z. H., Tammela, P., Strømme, M., & Nyholm, L. (2017). Cellulose-based supercapacitors: Material and performance considerations. *Advanced Energy Materials*, *7*, 1700130.

Yuan, L., Xiao, X., Ding, T., Zhong, J., Zhang, X., Shen, Y., Hu, B., Huang, Y., Zhou, J., & Wang, Z. L. (2012) Paper-based supercapacitors for self-powered nanosystems. *Angewandte Chemie International Edition*, *51*, 4934–4938.

Zhang, L.-L., Li, H.-H., Fan, C.-Y., Wang, K., Wu, X.-L., Sun, H.-Z., & Zhang, J.-P. (2015). A vertical and cross-linked $Ni(OH)_2$ network on cellulose-fiber covered with graphene as a binder-free electrode for advanced asymmetric supercapacitors. *Journal of Materials Chemistry A*, *3*, 19077–19084.

Zheng, Q., Cai, Z., Ma, Z., & Gong, S. (2015). Cellulose nanofibril/reduced graphene oxide/carbon nanotube hybrid aerogels for highly flexible and all-solid-state supercapacitors. *ACS Applied Materials & Interfaces*, *7*, 3263−3271.

Zhou, Q., Ye, X., Wan, Z., & Jia, C. (2015). A three-dimensional flexible supercapacitor with enhanced performance based on lightweight, conductive graphene-cotton fabric electrode. *Journal of Power Sources*, *296*, 186–196.

GRAPHICAL ABSTRACT